International Journal of Mechanical Sciences 70 (2013) 146–154

Contents lists available at SciVerse ScienceDirect

International Journal of Mechanical Sciences

journal homepage: www.elsevier.com/locate/ijmecsci

Thermophoresis and Brownian motion effects on MHD boundary-layer flow of a nanofluid in the presence of thermal stratification due to solar radiation

R. Kandasamy*, I. Muhaimin, Radiah Mohamad

Research Centre for Computational Mathematics, FSTPi, Universiti Tun Hussein Onn Malaysia, Johor, Malaysia

ARTICLE INFO

Article history:
Received 9 July 2011
Received in revised form
23 January 2013
Accepted 8 March 2013
Available online 21 March 2013

Keywords:
Solar radiation
Brownian motion;
Magnetic effect
Nanofluids;
Thermophoresis
Thermal stratification

ABSTRACT

The problem of laminar fluid flow which results from the stretching of a vertical surface with variable stream conditions in a nanofluid due to solar radiation has been investigated numerically. The model used for the nanofluid incorporates the effects of Brownian motion and thermophoresis with thermal stratification in the presence of magnetic field. The symmetry groups admitted by the corresponding boundary value problem are obtained by using a special form of Lie-group transformations viz. scaling group of transformations. An exact solution is obtained for translation symmetry and numerical solutions for scaling symmetry. This solution depends on a Lewis number, magnetic field, Brownian motion parameter, thermal stratification parameter and thermophoretic parameter. The conclusion is drawn that the flow field and temperature and nanoparticle volume fraction profiles are significantly influenced by these parameters.

1. Introduction

Energy plays an important role in the development of human society. However, over the past century, the fast development of human society leads to the shortage of global energy and the serious environmental pollution. All countries of the world have to explore new energy sources and develop new energy technologies to find the rode to sustainable development. Solar energy as the renewable and environmental friendly energy, it has produced energy for billions of years. Solar energy that reaches the earth is around 4×1015 MW, it is 2000 times as large as the global energy consumption. Thus the utilization of solar energy and the technologies of solar energy materials attract much more attention. Nano-materials as a new energy material, since its particle size is the same as or smaller than the wavelength of de Broglie wave and coherent wave. Therefore, nanoparticle becomes to strongly absorb and selectively absorb incident radiation. Based on the radiation and Brownian motion properties of nanoparticle, the utilization of nanofluids in solar thermal system becomes the new study hotspot.

Solar energy is one of the best sources of renewable energy with minimal environmental impact. Solar power is very important in our daily uses and it is a natural way of obtaining heat, electricity and water with the help from the nature. In near future we will be forced to switch our powering ways to keep the above mentioned necessities and conveniences. As we will face some fossil fuels crisis, the solar power is a renewable source of energy which never consumes. The radiation that comes from solar energy along with the resultant solar energized resources such as wave power, wind, biomass and hydroelectricity all give an explanation for most of the accessible renewable energy that is present on earth. Solar energy is currently one kind of important resource for clean and renewable energy, and is widely investigated in many fields. In order to increase the operating temperature and thermodynamic efficiency, concentrated solar radiation is normally used to heat the working fluid in solar thermal power system [28,26] and other industrial engineering. Solar thermal power system [25] is a very promising and challenging technology for its high operating temperature and thermodynamic efficiency. The heat losses of natural convection and radiation play an important role in heat absorption process of the heat receiver. Clausing [9] analyzed the convective losses from cavity solar central receivers. Dehghan and Behnia [10] researched combined natural convection conduction and radiation heat transfer in a discretely heated open cavity. Muftuoglu and Bilgen [23] simulated heat transfer in inclined rectangular receivers for concentrated solar radiation. In addition, the solar selective coatings are usually used to increase the absorption efficiency of the receiver, and Kennedy [14] reported solar selective absorber materials in a wide temperature range. The nanofluid is a colloidal suspension with nanoparticles dispersed uniformly in a base fluid and has many unique characteristics in thermal engineering fields.

A nanofluid is a new class of heat transfer fluids that contain a base fluid and nanoparticles. The use of additives is a technique

* Corresponding author. Tel.: +60 17 7977 259; fax: +60 74 5360 51.
E-mail address: future990@gmail.com (R. Kandasamy).

0020-7403/$ - see front matter © 2013 Elsevier Ltd. All rights reserved.
http://dx.doi.org/10.1016/j.ijmecsci.2013.03.007

Nomenclature

B_0	magnetic field strength
C	nanoparticles volume fraction
C_f	skin-fraction coefficient
C_w	nanoparticle volume fraction at the wall
C_∞	ambient nanoparticle volume fraction
c_p	specific heat at constant pressure
D_B	Brownian diffusion coefficient
D_T	thermophoretic diffusion coefficient
f	dimensionless stream function
g	acceleration due to gravity
k	thermal conductive
Le	Lewis number
M	magnetic parameter
Nb	Brownian motion parameter
n	thermal stratification parameter
Nt	thermophoresis parameter
Nr	buoyancy ratio
Pr	Prandtl number
P	pressure
Rax	local Rayleigh number
S	suction/injection parameter
T	temperature of the fluid
T_w	temperature at the wall
T_∞	ambient temperature
$\overline{v}$	velocity vector
u,v	velocity components along x- and y-axes
$U(x)$	uniform velocity of the free stream flow
V_0	velocity of suction/injection

Greek symbols

α	thermal conductivity
β	coefficient of thermal expansion
θ	dimensionless temperature
φ	dimensionless nanoparticle volume fraction
η	similarity variable
μ	dynamic viscosity
σ	electric conductivity of the fluid
ρ_f	density of the base fluid
ρ_P	nanoparticle mass density
$(\rho\ c)_f$	heat capacity of the base fluid
$(\rho\ c)_P$	effective heat capacity of the nanoparticle material
τ	heat capacity ratio
ν	kinematic viscosity
ψ	stream function

applied to enhance the heat transfer performance of base fluids. The thermal conductivity of the ordinary heat transfer fluids is not adequate to meet today's cooling rate requirements. Nanofluids have been shown to increase the thermal conductivity and convective heat transfer performance of the base liquids. One of the possible mechanisms for anomalous increase in the thermal conductivity of nanofluids is the Brownian motions of the nanoparticles inside the base fluids. The addition of small particles causes scattering of the incident radiation allowing higher levels of absorption within the fluid. A recent development in solar thermal collectors, proposed by Todd et al. [27], is the use of nanofluids to directly absorb solar radiation. The term nanofluid applies to colloidal suspensions of nanoparticles, which have been the subject of much recent study for their potentially enhanced thermal transport characteristics. Adding nanoparticles in suspension to a base liquid can drastically alter the optical properties of the fluid. The optical properties of the effective fluid are highly dependent on the particle shape, particle size, and the optical properties of the base fluid and particles themselves [16,8]). In order to fully understand the effects of suspending nanoparticles within a base fluid the complete optical properties of the base fluid are needed. Nanofluids are engineered colloidal suspensions of nanoparticles in water and exhibit a very significant enhancement of the boiling critical heat flux at modest nanoparticle concentrations. They are also used in other electronic applications which use microfluidic applications.

Magnetic nanofluid is a unique material that has both the liquid and magnetic properties. Many of the physical properties of these fluids can be tuned by varying magnetic field. The characteristic feature of nanofluids is thermal conductivity enhancement, a phenomenon observed by Masuda et al. [22]. This phenomenon suggests the possibility of using nanofluids in advanced nuclear systems [5]. A comprehensive survey of convective transport in nanofluids was made by Buongiorno [6], who says that a satisfactory explanation for the abnormal increase of the thermal conductivity and viscosity is yet to be found. He focused on the further heat transfer enhancement observed in convective situations. Kuznetsov and Nield [18] have examined the influence of nanoparticles on natural convective boundary-layer flow past a vertical plate, using a model in which Brownian motion and thermophoresis are accounted for. The authors have assumed the simplest possible boundary conditions, namely those in which both the temperature and the nanoparticle fraction are constant along the wall. Further, Nield and Kuznetsov [24] have studied the Cheng–Minkowycz [7] problem of natural convection past a vertical plate, in a porous medium saturated by a nanofluid. The model used for the nanofluid incorporates the effects of Brownian motion and thermophoresis. Tzou [29], Buongiorno [6], and Brenner and Bielenberg [4] considered Brownian motion and thermophoresis of nanoparticles and presented another equation for volume fraction of nanoparticles and investigated the thermal instability in nanofluids.

Recently, Kuznetsov and Nield [17,19] and Nield and Kuznetsov [20] have examined an analytical treatment of double-diffusive nanofluid convection in a porous medium. The model used for the nanofluid incorporates the effects of Brownian motion and thermophoresis, while the base fluid of the nanofluid is itself a binary fluid such as salty water whereas in the present study we considered the combined effects of Brownian motion and thermophoresis with thermal stratification in the presence of copper nanofluid due to solar radiation. The thermal conductivity of the ordinary heat transfer fluids is not adequate to meet today's cooling rate requirements. Nanofluids have been shown to increase the thermal conductivity and convective heat transfer performance of the base liquids. One of the possible mechanisms for the anomalous increase in the thermal conductivity of nanofluids is the Brownian motions of the nanoparticles inside the base fluids. The study of heat and mass transfer with thermophoresis particle deposition in the presence of temperature-dependent fluid viscosity is of great practical importance to engineers and scientists because of its almost universal occurrence in many branches of science and engineering. Thermophoresis particle deposition with Brownian motion principle in the presence of temperature-dependent viscosity is utilized to manufacture graded index silicon dioxide and germanium dioxide optical fiber preforms used in the field of communications. For the porous

medium the Darcy model has been employed. Thermal stratification phenomena are very common in pool type reactor systems, such as the liquid-salt cooled advanced high temperature reactor and liquid-metal cooled fast reactor systems such as the sodium fast reactor. It is important to accurately predict the temperature and density distributions both for design optimization and accident analysis.

In the present study we considered the combined effects of Brownian motion and thermophoresis in the presence of thermal stratification due to solar radiation to get the gradient of nanoparticles' volume fraction. Using Lie-group analysis, three-dimensional, unsteady, laminar boundary-layer equations of non-Newtonian fluids were studied by Yurusoy and Pakdemirli [30,31]. Using Lie-group analysis, they obtained two different reductions to ordinary differential equations. They studied the effects of a moving surface with vertical suction or injection through the porous surface and also analyzed the exact solution of boundary-layer equations of a special non-Newtonian fluid over a stretching sheet by the method of Lie-group analysis. Yurusoy et al. [32] investigated the Lie-group analysis of creeping flow of a second grade fluid. They constructed an exponential type of exact solution using the translation symmetry and a series type of approximate solution using the scaling symmetry and also discussed some boundary value problems. The objective of the present study is to analyze the development of the steady boundary-layer flow, heat transfer and nanoparticle volume fraction over a stretching surface in a nanofluid for various parameters using scaling group of transformations viz., Lie-group transformations.

2. Mathematical analysis

We consider a two-dimensional problem. We select a coordinate frame in which the x-axis is aligned vertically upwards. We consider a vertical plate at $y=0$. A uniform transverse magnetic field of strength $\overline{B}_0$ is applied parallel to the y-axis. It is assumed that the induced magnetic field, the external electric field and the electric field due to the polarization of charges are negligible. Far away from the vertical plate, both the surroundings and the Newtonian and absorbing fluid are maintained at a constant temperature T_∞. The porous medium is assumed to be transparent and in thermal equilibrium with the fluid. Both the fluid and the porous medium are opaque for self-emitted thermal radiation. Also, the solar radiation is a collimated beam that is normal to the plate. Due to the heating of the absorbing fluid and the vertical plate by solar radiation, heat is transferred from the plate to the surroundings. As mentioned before, the working fluid is assumed to have heat absorption properties. In this situation, the porous medium absorbs the incident solar radiation and transmits it to the working fluid by convection. At this boundary the temperature T and the nanoparticle fraction ϕ take constant values T_w and ϕ_w, respectively. The ambient values, attained as y tends to infinity, of T and ϕ are denoted by T_∞ and ϕ_∞, respectively.

The Oberbeck–Boussinesq approximation is employed. The following four field equations embody the conservation of total mass, momentum, thermal energy, and nanoparticles, respectively. The field variables are the velocity $\mathbf{v}$, the temperature T and the nanoparticle volume fraction ϕ.

$$\nabla.\overline{v}=0 \tag{1}$$

$$\rho_f\left(\frac{\partial\overline{v}}{\partial t}+\overline{v}.\nabla\overline{v}\right)=-\nabla p+\nabla\mu.\nabla\overline{v}-\left(\sigma\overline{B}_0^2+\frac{\nu}{K}\right)\overline{v}+\mu\nabla^2\overline{v}+[C\rho_p+(1-C)\{\rho_f(1-\beta(T-T_\infty))\}]\overline{g} \tag{2}$$

$$(\rho c)_f\left(\frac{\partial T}{\partial t}+\overline{v}.\nabla T\right)=k\nabla^2T+(\rho c)_p\left[D_B\nabla C.\nabla T+\left(\frac{D_T}{T_\infty}\right)\nabla T.\nabla T\right]-\nabla.q_{rad}^{'} \tag{3}$$

$$\frac{\partial C}{\partial t}+\overline{v}.\nabla C=D_B\nabla^2C+\frac{D_T}{T_\infty}\nabla^2T \tag{4}$$

We write $\overline{v}=(u,v)$.

Here ρ_f is the density of the base fluid, $\overline{B}_0$ is a constant magnetic field of strength, σ is the electric conductivity, K is the permeability of the porous medium, $q_{rad}^{'}$ is the applied absorption radiation heat transfer per unit area, μ, k and β are the density, viscosity, thermal conductivity and volumetric volume expansion coefficient of the nanofluid, respectively, while ρ_p is the density of the particles. The gravitational acceleration is denoted by $\overline{g}$. The coefficients that appear in Eqs. (3) and (4) are the Brownian diffusion coefficient D_B and the thermophoretic diffusion coefficient D_T. Details of the derivation of Eqs. (3) and (4) are given in the paper by Buongiorno [6] and Nield and Kuznetsov [24]. The boundary conditions are taken to be

$$u=U(x),\quad v=V(x),\quad C=C_w,\quad T=T_w \text{ at } y=0;\quad u=0,\quad C=C_\infty,\quad T\to T_\infty=(1-n)T_o+nT_w \text{ as } \overline{y}\to\infty \tag{5}$$

Here n is a constant, such that $0\le n<1$. The n defined as above is equal to $m_1/(1+m_1)$ [1] where m_1 is a constant and n refers to thermal stratification parameter. T_o is a constant reference temperature say $T_\infty(0)$. The suffixes w and ∞ denote surface and ambient conditions.

We consider a steady state flow.

In keeping with the Oberbeck–Boussinesq approximation and an assumption that the nanoparticle concentration is dilute, and with a suitable choice for the reference pressure, we can linearize the momentum equation and write Eq. (2) as

$$\rho_f\left(\frac{\partial\overline{v}}{\partial t}+\overline{v}.\nabla\overline{v}\right)=-\nabla p+\nabla\mu.\nabla\overline{v}+\mu\nabla^2\overline{v}+\left[(\rho_p-\rho_{f_\infty})(C-C_\infty)+(1-C_\infty)\rho_{f_\infty}\beta(T-T_\infty)\right]\overline{g}-\left(\sigma\overline{B}_0^{\,2}+\frac{\nu}{K}\right)\overline{v} \tag{6}$$

We now make the standard boundary-layer approximation, based on a scale analysis, and write the governing equations

$$\frac{\partial u}{\partial x}+\frac{\partial v}{\partial y}=0 \tag{7}$$

$$\frac{\partial p}{\partial x}=\mu\frac{\partial^2u}{\partial y^2}+\frac{\partial\mu}{\partial T}\frac{\partial T}{\partial y}\frac{\partial u}{\partial y}-\rho_f\left(u\frac{\partial u}{\partial x}+v\frac{\partial u}{\partial y}\right)+\left[(1-C_\infty)\rho_{f_\infty}\beta g(T-T_\infty)-(\rho_p-\rho_{f_\infty})g(C-C_\infty)\right]-\left(\sigma B_0^{\,2}+\frac{\nu}{K}\right)u \tag{8}$$

$$\frac{\partial p}{\partial y}=0 \tag{9}$$

$$u\frac{\partial T}{\partial x}+v\frac{\partial T}{\partial y}=\alpha\frac{\partial^2T}{\partial y^2}+\tau\left[D_B\frac{\partial C}{\partial y}\frac{\partial T}{\partial y}+\frac{D_T}{T_\infty}\left(\frac{\partial T}{\partial y}\right)^2\right]-\frac{1}{(\rho c)_f}\frac{\partial q''_{rad}}{\partial y} \tag{10}$$

$$u\frac{\partial C}{\partial x}+v\frac{\partial C}{\partial y}=D_B\frac{\partial^2C}{\partial y^2}+\frac{D_T}{T_\infty}\frac{\partial^2T}{\partial y^2} \tag{11}$$

where u and v are the velocity components along the x- and y-axes, respectively, $\alpha=(k/(\rho c)_f)$ is the thermal diffusivity of the fluid, ν is the kinematic viscosity coefficient and $\tau=(\rho c)_p/(\rho c)_f$.

Using Rosseland approximation for radiation [3] we can write that $q''_{rad}=-(4\sigma_1/3k^*)(\partial T^4/\partial y)$ is the applied absorption radiation heat transfer where σ_1 is the Stefan–Boltzman constant, k^* is the absorption coefficient.

The stream wise velocity and the suction/injection velocity are taken as

$$U(x)=cx^m,\quad V(x)=f_w x^{(m-1)/2} \tag{12}$$

Here $c>0$ is constant, T_w is the wall temperature, the power-law exponent m is also constant. In this study we take $c=1$.

The temperature-dependent fluid viscosity is given by [2]

$\mu = \mu^*[a+b(T_w-T)]$

where μ^* is the constant value of the coefficient of viscosity far away from the sheet and a,b are constants and $b(>0)$. For a viscous fluid, Ling and Dybbs [21] suggested a viscosity dependence on temperature T of the form $\mu = \mu_\infty/[1+\gamma(T-T_\infty)]$ where c is a thermal property of the fluid and μ_∞ is the viscosity away from the hot sheet. This relation does not differ at all with our formulation. The range of temperature, i.e. (T_w-T_∞) °C studied here is (0–23) °C.

One can eliminate p from Eqs. (8) and (9) by cross-differentiation. At the same time one can introduce a stream function ψ defined by

$$u = \frac{\partial \psi}{\partial y}, \quad v = -\frac{\partial \psi}{\partial x}, \quad \theta = \frac{T-T_\infty}{T_w-T_\infty}, \quad \text{and} \quad \phi = \frac{C-C_\infty}{C_w-C_\infty} \tag{13}$$

Using the relations (7) into Eqs. (2)–(4), we obtain

$$\frac{\partial \psi}{\partial y}\frac{\partial^2 \psi}{\partial x \partial y} - \frac{\partial \psi}{\partial x}\frac{\partial^2 \psi}{\partial y^2} = -\zeta\, \nu^* \frac{\partial \theta}{\partial y}\frac{\partial^2 \psi}{\partial y^2} + \nu^*[a+\zeta(1-\theta)]\frac{\partial^3 \psi}{\partial y^3}$$
$$+(1-\phi_\infty)\rho_{f_\infty}\beta g\theta\Delta\theta - (\rho_p-\rho_{f_\infty})g\phi\Delta\phi - \frac{\nu}{K}\frac{\partial \psi}{\partial y} - \frac{\sigma {B_0}^2}{\rho}\frac{\partial \psi}{\partial y} \tag{14}$$

$$\frac{\partial \psi}{\partial y}\frac{\partial \theta}{\partial x} - \frac{\partial \psi}{\partial x}\frac{\partial \theta}{\partial y} = \alpha\frac{\partial^2 \theta}{\partial y^2} + \tau\left[D_B\frac{\partial \phi}{\partial y}\frac{\partial \theta}{\partial y} + \frac{D_T}{T_\infty}\left(\frac{\partial \theta}{\partial y}\right)^2\right] + \frac{4}{3}N\left[(C_T+\theta)^3\frac{\partial \theta}{\partial y}\right]' \tag{15}$$

$$\frac{\partial \psi}{\partial y}\frac{\partial \phi}{\partial x} - \frac{\partial \psi}{\partial x}\frac{\partial \phi}{\partial y} = D_B\frac{\partial^2 \phi}{\partial y^2} + \frac{D_T}{T_\infty}\frac{\partial^2 \theta}{\partial y^2} \tag{16}$$

$$\frac{\partial \psi}{\partial y} = x^m, \quad \frac{\partial \psi}{\partial x} = -f_w x^{m-1/2}, \quad C = C_w, \quad T = T_w \text{ at } y = 0;$$
$$\frac{\partial \psi}{\partial y} \to 0, \quad C = C_\infty, \quad T \to T_\infty = (1-n)T_o + nT_w \text{ as } y \to \infty \tag{17}$$

where

$$\zeta = b(T_w-T_\infty), \quad \nu^* = \frac{\mu^*}{\rho}, \quad \tau = -\frac{k(T_w-T_\infty)}{T_r}$$

We now introduce the simplified form of Lie-group transformations namely, the scaling group of transformations,

$$\Gamma: x^* = xe^{\varepsilon\alpha_1}, \quad y^* = ye^{\varepsilon\alpha_2}, \quad \psi^* = \psi e^{\varepsilon\alpha_3}, \quad u^* = ue^{\varepsilon\alpha_4},$$
$$v^* = ve^{\varepsilon\alpha_5}, \quad \theta^* = \theta e^{\varepsilon\alpha_6}, \quad \phi^* = \phi e^{\varepsilon\alpha_7} \tag{18}$$

Eq. (18) may be considered as a point-transformation which transforms co-ordinates $(x, y, \psi, u, v, \theta, \phi)$ to the co-ordinates $(x^*, y^*, \psi^*, u^*, v^*, \theta^*, \phi^*)$.

Substituting Eq. (18) in Eqs. (14)–(16) we get

$$e^{\varepsilon(\alpha_1+2\alpha_2-2\alpha_3)}\left(\frac{\partial \psi^*}{\partial y^*}\frac{\partial^2 \psi^*}{\partial x^* \partial y^*} - \frac{\partial \psi^*}{\partial x^*}\frac{\partial^2 \psi^*}{\partial y^{*2}}\right) = -\zeta\nu^* e^{\varepsilon(3\alpha_2-\alpha_3-\alpha_6)}\left(\frac{\partial \theta^*}{\partial y^*}\frac{\partial^2 \psi^*}{\partial y^{*2}}\right)$$
$$-\left(\frac{\sigma B_0^2}{\rho}+\frac{\nu}{K}\right)e^{\varepsilon(\alpha_2-\alpha_3)}\frac{\partial \psi^*}{\partial y^*} + \nu^*[a+\zeta]e^{\varepsilon(3\alpha_2-\alpha_3)}\frac{\partial^3 \psi^*}{\partial y^{*3}}$$
$$-\zeta\nu^* e^{\varepsilon(3\alpha_2-\alpha_3-\alpha_6)}\theta^*\frac{\partial^3 \psi^*}{\partial y^{*3}}$$
$$+e^{-\varepsilon\alpha_6}(1-\phi_\infty)\rho_{f\infty}\beta g\theta^*\Delta\theta - e^{-\varepsilon\alpha_7}(\rho_p-\rho_{f\infty})g\phi^*\Delta\phi \tag{19}$$

$$e^{\varepsilon(\alpha_1+\alpha_2-\alpha_3-\alpha_6)}\left(\frac{\partial \psi^*}{\partial y^*}\frac{\partial \theta^*}{\partial x^*} - \frac{\partial \psi^*}{\partial x^*}\frac{\partial \theta^*}{\partial y^*}\right)$$
$$= \alpha e^{\varepsilon(2\alpha_2-\alpha_6)}\frac{\partial^2 \theta^*}{\partial y^{*2}} + e^{\varepsilon(2\alpha_2-\alpha_6)}\frac{4}{3}N\left[(C_T+\theta)^3\frac{\partial \theta^*}{\partial y^*}\right]'$$
$$+\tau\left[D_B e^{\varepsilon(2\alpha_2-\alpha_6-\alpha_7)}\frac{\partial \varphi^*}{\partial y^*}\frac{\partial \theta^*}{\partial y^*} + e^{\varepsilon(2\alpha_2-2\alpha_6)}\frac{D_T}{T_\infty}\left\{\frac{\partial \theta^*}{\partial y^*}\right\}^2\right] \tag{20}$$

$$e^{\varepsilon(\alpha_1+\alpha_2-\alpha_3-\alpha_7)}\left(\frac{\partial \psi^*}{\partial y^*}\frac{\partial \phi^*}{\partial x^*} - \frac{\partial \psi^*}{\partial x^*}\frac{\partial \phi^*}{\partial y^*}\right) = D_B e^{\varepsilon(2\alpha_2-\alpha_7)}\frac{\partial^2 \phi^*}{\partial y^{*2}}$$
$$+\frac{D_T}{T_\infty}e^{\varepsilon(2\alpha_2-\alpha_6)}\frac{\partial^2 \theta^*}{\partial y^{*2}} \tag{21}$$

The system will remain invariant under the group of transformations Γ, we would have the following relations among the parameters, namely

$\alpha_1+2\alpha_2-2\alpha_3 = 3\alpha_2-\alpha_3 = \alpha_2-\alpha_3 = -\alpha_6 = -\alpha_7$;
$\alpha_1+\alpha_2-\alpha_3-\alpha_6 = 2\alpha_2-\alpha_6 = 2\alpha_2-\alpha_6-\alpha_7 = 2\alpha_2-2\alpha_6$ and
$\alpha_1+\alpha_2-\alpha_3-\alpha_7 = 2\alpha_2-\alpha_7 = 2\alpha_2-\alpha_6$

These relations $3\alpha_2-\alpha_3 = \alpha_2-\alpha_3$ give the value $\alpha_2 = 0$

Hence, $\alpha_1+2\alpha_2-2\alpha_3 = 3\alpha_2-\alpha_3$ gives $\alpha_6 = \alpha_7 = 0$, $\alpha_2 = (1/4)\alpha_1 = (/13)\alpha_3$.

The boundary conditions yield $\alpha_4 = m\alpha_1 = (1/2)\alpha_1$, $\alpha_5 = ((m-1)/2)\alpha_1 = -(1/4)\alpha_1$ (as $m = (1/2)$)

In view of these, the boundary conditions become

$$\frac{\partial \psi^*}{\partial y^*} = x^{*(1/2)}, \quad \frac{\partial \psi^*}{\partial x^*} = -f_w x^{*(-(1/4))}, \quad C = C_w, \quad T = T_w \text{ at } y^* = 0 \text{ and}$$
$$\frac{\partial \psi^*}{\partial y^*} \to 0, \quad C = C_\infty, \quad T \to T_\infty = (1-n)T_o + nT_w \text{ as } y^* \to \infty \tag{22}$$

The set of transformations Γ reduces to

$$x^* = xe^{\varepsilon\alpha_1}, \quad y^* = ye^{\varepsilon(\alpha 1/4)}, \quad \psi^* = \psi e^{\varepsilon(3\alpha 1/4)}, \quad u^* = ue^{\varepsilon(\alpha 1/2)},$$
$$v^* = ve^{-\varepsilon(\alpha 1/4)}, \quad \theta^* = \theta, \quad \phi^* = \phi$$

Expanding by Taylor's method in powers of ε and keeping terms up to the order ε we get

$$x^*-x = x\varepsilon\alpha_1, \quad y^*-y = y\varepsilon\frac{\alpha_1}{4}, \quad \psi^*-\psi = \psi\varepsilon\frac{3\alpha_1}{4}, \quad u^*-u = u\varepsilon\frac{\alpha_1}{2},$$
$$v^*-v = -v\varepsilon\frac{\alpha_1}{4}, \quad \theta^*-\theta = \phi^*-\phi = 0$$

From the above equations we get

$$y^*x^{*(-1/4)} = \eta, \quad \psi^* = x^{*(3/4)}f(\eta), \quad \theta^* = \theta(\eta), \quad \phi^* = \phi(\eta) \tag{23}$$

With the help of these relations, Eqs. (19)–(21) become

$$(a+\zeta)f''' - \zeta\theta f''' - \zeta\theta' f'' - \frac{1}{2}f'^2 - (M+\lambda)f' + \frac{3}{4}ff'' + \zeta\, Rax\,(\theta - Nr\phi) = 0 \tag{24}$$

$$\theta'' + \frac{4}{3}N\left[(C_T+\theta)^3\theta'\right]' + \frac{3}{4}f\theta' - \frac{3}{4}\left(\theta + \frac{n}{1-n}\right)f' + Nb\theta'\phi' + Nt\theta'^2 = 0 \tag{25}$$

$$\phi'' + \frac{3}{4}Lef\phi' + \frac{Nt}{Nb}\theta'' = 0 \tag{26}$$

The boundary conditions take the following form:

$$f' = 1, \quad f = -\frac{4f_w}{3}, \quad \theta = \phi = 1 \text{ at } \eta = 0 \text{ and } f' \to 0, \quad \theta \to 0,$$
$$\phi \to 0 \text{ as } \eta \to \infty \tag{27}$$

where $Pr = \nu^*/\alpha^*$ is the Prandtl number, $Rax = ((1-\phi_\infty)\beta g)/b\nu^*\alpha^*$ is the local Rayleigh number, $Nr = ((\rho_p-\rho_{f_\infty})\Delta\phi)/\rho_{f_\infty}\beta\Delta\theta(1-\phi_\infty)$ is the buoyancy ratio, $Nb = ((\rho c)_p D_B\Delta\phi)/\alpha(\rho c)_f$ is the Brownian motion parameter, $Nt = ((\rho c)_p D_T\Delta\theta)/\alpha(\rho c)_f T_\infty$ is the thermophoresis parameter, $\lambda = \nu/K\rho_f$ is the porous media parameter, $M = \sigma\, B_0^2 U/\rho_f$ is the magnetic parameter, $Le = \nu^*/D$ is the Lewis number, $N = 4\sigma_1\theta^3/((\rho c_p)_f k^*)$ is the conduction radiation parameter and $C_T = T_\infty/(T_w-T_\infty)$ is the temperature ratio, where C_T assumes very small values by its definition as T_w-T_∞ is very large compared to T_∞. In the present study, it is assigned the value 0.01.

The boundary conditions take the following forms:

$$f' = 1, \quad f = S, \quad \theta = \phi = 1, \text{ at } \eta^* = 0 \text{ and } f' \to 0, \quad \theta \to 0,$$
$$\phi \to 0 \text{ as } \eta^* \to \infty \tag{28}$$

where $S=-(4/3)f_w$, $S>0$ corresponds to suction and $S<0$ corresponds to injection whereas f_w is the velocity of suction if $f_w<0$ and injection if $f_w>0$.

3. Numerical solution

The set of non-linear ordinary differential equations (24)–(26) with boundary conditions (28) have been solved by using the Runge Kutta Gill algorithm [12] with a systematic guessing of $f''(0)$, $\theta'(0)$ and $\phi'(0)$ by the shooting technique with until the boundary conditions at infinity $f''(\infty)$, $\theta'(\infty)$ and $\phi'(\infty)$ decay exponentially to zero. The computations were done by a program which uses a symbolic and computational computer language Matlab. The step size $\Delta\eta=0.001$ is used while obtaining the numerical solution with η_{max}, and accuracy to the fifth decimal place is sufficient for convergence. The value of η_∞ was found in each iteration loop by assignment statement $\eta_\infty=\eta_\infty+\Delta\eta$. The maximum value of η_∞, to each group of parameters N, n, M, Nr, Nb and Nt, determined when the values of unknown boundary conditions at $\eta=0$ not change to successful loop with error less than 10^{-7}. Effects of development of the steady boundary-layer flow, heat transfer and nanoparticle volume fraction over a porous vertical stretching surface in a nanofluid due to solar radiation are studied for different values of thermal stratification parameter, conduction radiation parameter, Brownian motion parameter, thermophoresis parameter and magnetic parameter. In the following section, the results are discussed in detail.

4. Results and discussion

Numerical analysis are carried out for $0.1\le N_b\le 3.0$, $0.1\le N_t\le 3.0$, $0.5\le M\le 5.0$, $0.1\le n<1.0$, $0.1\le N<5.0$, $C_T=0.01$ and $-2.0\le S\le 2.0$ (Fig. 1). To be realistic, in the case of nanofluid, the value of Lewis number, $10\le Le\le 100$ and the Prandtl number are chosen to be at $Pr=10$ (see [17,15]) which represents air at temperature 25 °C. The effect of buoyancy is significant for $Pr=10$ (air) due to the lower density of air that makes it more sensitive to the buoyancy forces. Local Rayleigh number $Rax(=3.0)>0$, buoyancy ratio $Nr=0.5$, Brownian motion parameter $N_b=0.5$, thermophoresis parameter $N_t=0.5$ effects in moving nanofluid are important in view of several physical problems (see [17,15]). Eqs. (24)–(26) subject to the boundary conditions (28) have been solved numerically for some values of the governing parameters Pr, n, M, N_r, N_b and N_t using Runge Kutta Gill algorithm with shooting technique. Neglecting the effects of Nb and Nt numbers, the results for the reduced Nusselt number $-\theta'(0)$ are compared with those obtained by Khan and Pop [15], Wang [33], and Gorla and Sidawi [13] for different values of Pr in Table 1. We notice that the comparison shows good agreement for each value of Pr. Therefore, we are confident that the present results are very accurate.

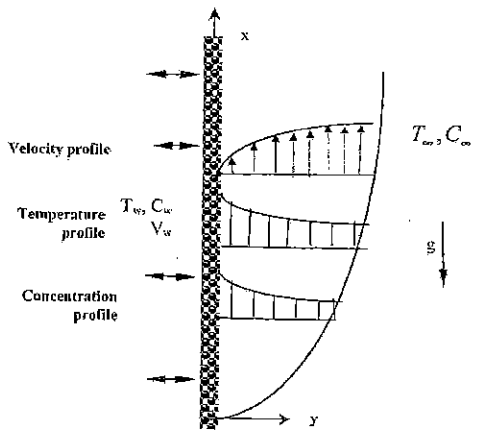

Fig. 1. Physical flow model and coordinate system over a vertical stretching surface.

In the absence of local Rayleigh number *Rax*, in order to ascertain the accuracy of our numerical results, the present study is compared with the available exact solution in the literature. The nanoparticle fraction profiles for Lewis number *Le* are compared with the available exact solution of khan and pop [15] are shown in Fig. 2a and b. It is observed that the agreements with the theoretical solution of nanoparticle fraction profiles are excellent. For a given *Nb* and *Nt*, it is clear that there is a fall in nanoparticle fraction with increasing the Lewis number. This is due to the fact that there would be a decrease of nanoparticle volume fraction boundary-layer thickness with the increase of Lewis number as one can see from Fig. 2a and b by comparing the curves with $Le=10$, $Le=20$ and $Le=30$.

Volume fraction of nanoparticles is a key parameter for studying the effect of nanoparticles on flow fields and temperature distributions. Thus Figs. 3 and 4 are prepared to present the effect of Brownian motion on temperature distribution and volume fraction of nanoparticle. Figs.3 and 4 illustrate the typical temperature and nanoparticle volume fraction profiles for various values of Brownian motion parameter, *Nb*. Temperature of the fluid increases and the nanoparticle volume fraction decreases with increase of *Nb*. It is interesting to note that Brownian motion of nanoparticles at the molecular and nanoscale levels is a key nanoscale mechanism governing their thermal behavior. In nanofluid systems, due to the size of the nanoparticles Brownian motion takes place which can affect the heat transfer properties. As the particle size scale approaches to the nano-meter scale, the particle Brownian motion and its effect on the surrounding liquids play an important role in heat transfer.

Figs. 5 and 6 display the effect of thermophoretic parameter *Nt* on temperature and nanoparticle volume fraction profiles. It is to note that the temperature of the fluid increases whereas the nanoparticle volume fraction decreases with increase of *Nt*. We notice that positive *Nt* indicates a cold surface, but is negative to a hot surface. For hot surfaces, thermophoresis tends to blow the nanoparticle volume fraction boundary layer away from the surface since a hot surface repels the sub-micron sized particles from it, thereby forming a relatively particle-free layer near the surface. As a consequence, the nanoparticle distribution is formed just outside. In particular, the effect of increasing the thermophoretic parameter *Nt* is limited to increasing slightly the wall slope of the nanoparticle volume fraction profiles but decreasing the nanoparticle volume fraction. This is true only for small values of Lewis number for which the Brownian diffusion effect is large compared to the convection effect. However, for large values of Lewis number, the diffusion effect is minimal compared to the convection effect and, therefore, the thermophoretic parameter *Nt* is expected to alter the nanoparticle volume fraction boundary layer

Table 1
Comparison of results for $-\theta'(0)$ with previous published works.

Pr	Khan and Pop [15]	Wang (1989) [33]	Gorla and Sidawi [13]	Present work
0.07	0.0663	0.0656	0.0656	0.0661 29
0.20	0.1691	0.1691	0.1691	0.1691 36
0.70	0.4539	0.4539	0.5349	0.4542 85
2.00	0.9113	0.9113	0.9113	0.9114 23
7.00	1.8954	1.8954	1.8905	0.8952 64
20.0	3.3539	3.3539	3.3539	3.3538 53
70.0	6.4621	6.4622	6.4622	6.4621 89

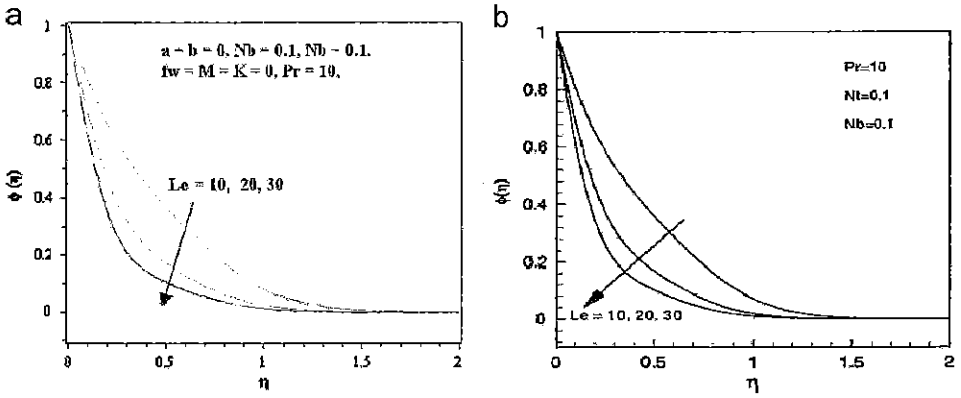

Fig. 2. (a) and (b) Comparison of the nanoparticles fraction profiles (present result—(a) with Khan and Pop [15]—(b).

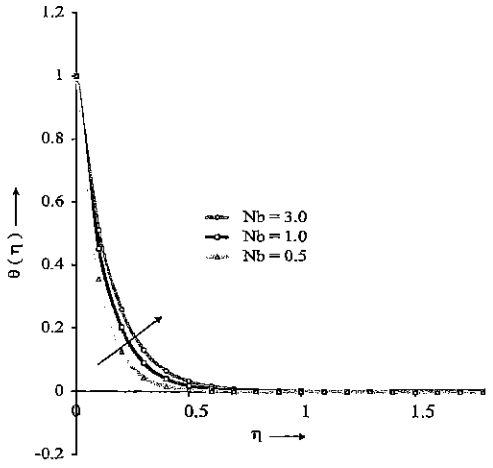

Fig. 3. Temperature profiles for various values of Nb when Pr= 10.0, Le=10.0, Nt=0.5, S=2.0, N=1.0, n.

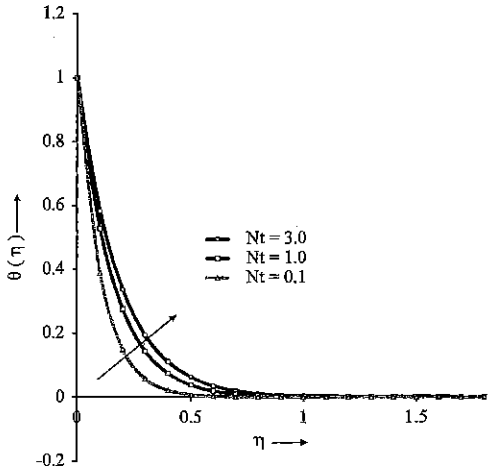

Fig. 5. Temperature profiles for various value of Nt when Pr=10.0, Le=10.0, Nb=0.5, S=2.0, N=1.0, Nr=0.5, M=1.0, n=0.5, a=ζ=1.0.

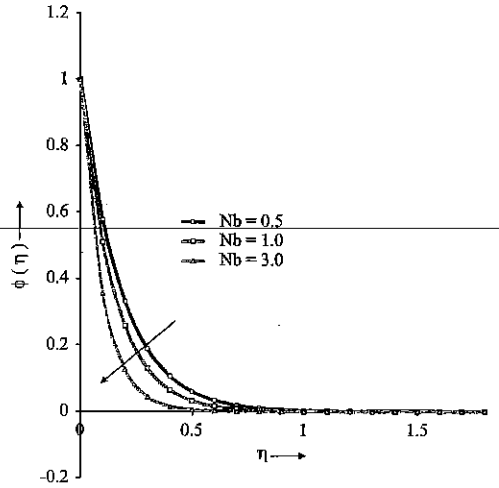

Fig. 4. Effect of Nb over the nanoparticle volume fraction profile when Pr=10.0, Le=10.0, Nt=0.5, S=2.0, N=1.0, n=0.5, a=ζ=1.0.

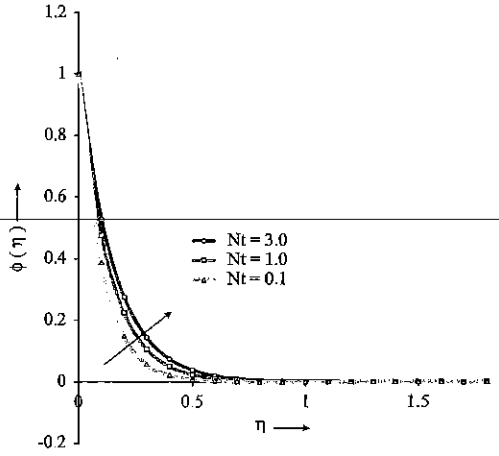

Fig. 6. Effect of Nt over the nanoparticle volume fraction profile when Pr=10.0, Le=10.0, Nb =0.5, S=2.0, N=1.0, Nr=0.5, M=1.0, n=0.5, a=ζ=1.0.

significantly. Although thermophoresis effect is important in natural convection of nanofluids, there are other parameters that may have effect, and should be considered. These effects include increase in effective viscosity of nanofluids due to the presence of nanoparticles and density variation due to variable volume fraction. More volume fraction of nanoparticles makes nanofluid much viscous and the mixture's convection takes place weaker, thus natural convective Nusselt number decreases due to high viscose fluid. On the other hand it is showed that the separation factor for common nanofluids is positive and density variation due to variable volume fraction of nanoparticles, called particulate buoyancy force, helps nanofluid to have strong convection heat transfer.

Figs. 7–9 depict the influence of the suction/injection parameter S on the velocity, temperature and nanoparticle volume fraction profiles in the boundary layer when the thermophoretic

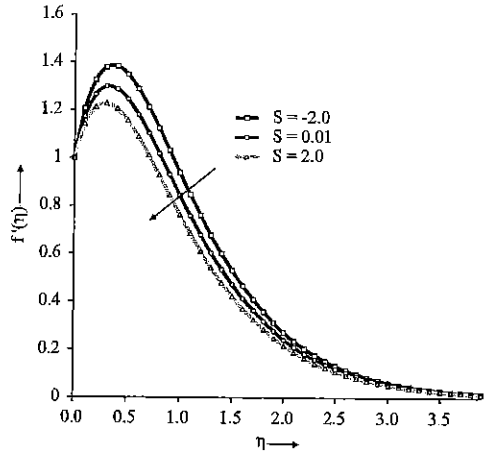

Fig. 7. Effect of suction/injection over the velocity profile when Pr=10.0, *Le*=10.0, *Nb*, *Nt*=0.5, *N*=1.0, *Nr*=0.5, *M*=1.0, *n*=0.5, *a*=*ζ*=1.0.

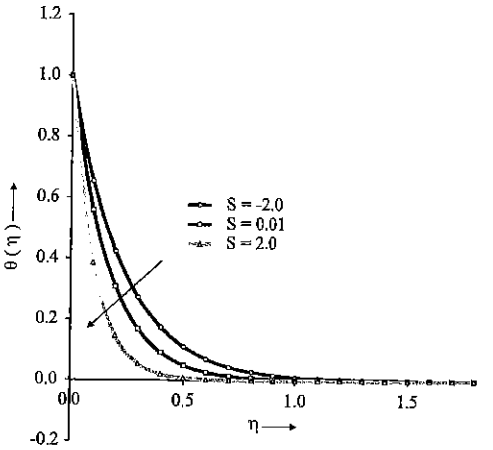

Fig. 8. Effect of suction/injection over the temperature profiles when Pr=10.0, *Le*=10.0, *Nb*, *Nt*=0.5, *N*=1.0, *Nr*=0.5, *M*=1.0, *n*=0.5, *a*=*ζ*=1.0.

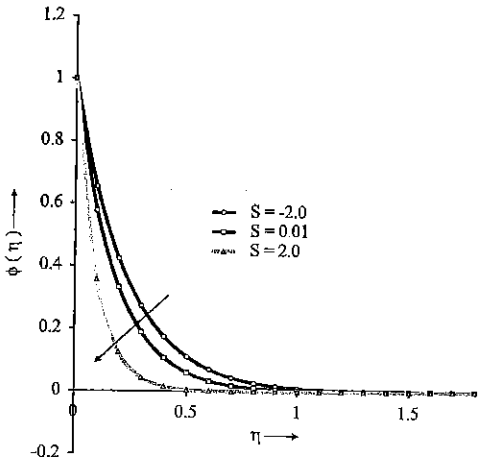

Fig. 9. Effect of suction/injection over the nanoparticle volume fraction profile when Pr=10.0, *Le*=10.0, *Nb*, *Nt*=0.5, *N*=1.0, *Nr*=0.5, *M*=1.0, *n*=0.5, *a*=*ζ*=1.0.

particle deposition is uniform, i.e. $Nt=0.5$. With the increasing value of the suction ($S>0$), the velocity is found to decrease (Fig.7), i.e. suction causes to decrease the velocity of the fluid in the boundary-layer region. In case of suction, the heated fluid is pushed towards the wall where the buoyancy forces can act to retard the fluid due to high influence of the Brownian motion effects. This effect acts to decrease the wall shear stress. Figs. 8 and 9 exhibit that the temperature $\theta(\eta)$ and nanoparticle volume fraction $\varphi(\eta)$ in boundary layer also decrease with the increasing suction parameter ($S>0$) (the fluid is of uniform thermophoretic particle deposition, i.e. $Nt=0.5$) (Pr=10.0 and $Nb=0.5$). The explanation for such behavior is that the fluid is brought closer to the surface and reduces the thermal and nanoparticle volume boundary-layer thickness in case of suction. As such then the presence of wall suction decreases velocity boundary-layer thicknesses but decreases the thermal and nanoparticle volume fraction boundary layers thickness, i.e. thins out the thermal and nanoparticle volume fraction boundary layers. However, the exact opposite behavior is produced by imposition of wall fluid blowing or injection. These behaviors are also clear from Figs.7 to 9. The samples of velocity, temperature and the nanoparticle volume fraction profiles are given in Figs. 7–9, respectively. These profiles satisfy the far field boundary conditions (28) asymptotically, which support the numerical results obtained.

Figs. 10 and 11 present typical profiles for velocity and temperature for different values of magnetic parameter. Due to the uniform thermophoresis particle deposition, it is clearly shown that the velocity of the fluid decreases and the temperature of the fluid increases whereas the nanoparticle volume fraction of the fluid is not significant with increase of the strength of magnetic field. The effects of a transverse magnetic field to an electrically conducting fluid give rise to a resistive-type force called the Lorentz force. This force has the tendency to slow down the motion of the fluid and to increase its temperature profiles. This result qualitatively agrees with the expectations, since magnetic field exerts retarding force on the natural convection flow. Application of a magnetic field moving with the free stream has the tendency to induce a motive force which decreases the motion of the fluid and increases its boundary layer.

Fig. 12 illustrates typical profile for temperature for different values of thermal stratification parameter in the case of uniform magnetic field. It is clearly shown that the temperature of the fluid decreases whereas nanoparticle volume fraction profiles are not significant with increase of the strength of thermal stratification. In particular, the temperature of the fluid gradually changes from higher value to the lower value only when the strength of thermal stratification is higher than the thermophoresis and Brownian motion parameters. For heat transfer characteristics mechanism, interesting result is the large distortion of the temperature field caused for $0.9\leq n<1$. Negative value of the temperature profile is

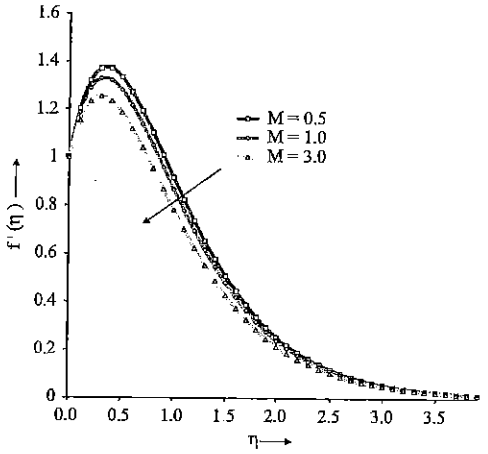

Fig. 10. Magnetic effect over the velocity profiles when Pr=10.0, *Le*=10.0, *Nb*, *Nt*=0.5, *S*=2.0, *N*=1.0, *a*=*ζ*=1.0, *Nr*=0.5, *n*=0.5.

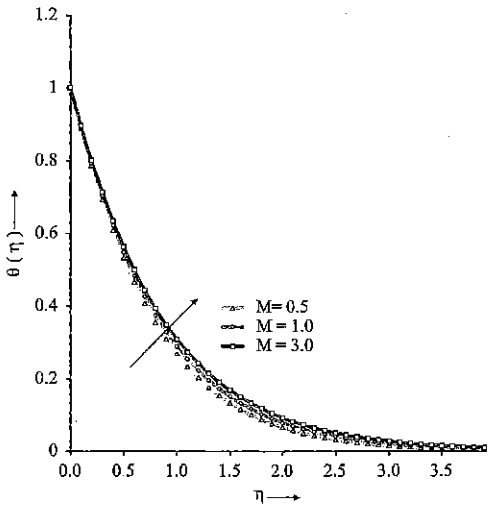

Fig. 11. Magnetic effect over the temperature profiles when Pr=10.0, *Le*=10.0, *Nb*, *Nt*=0.5 *S*=2.0, *a*=*ζ*=1.0, *Nr*=0.5, *n*=0.5, *N*=1.0.

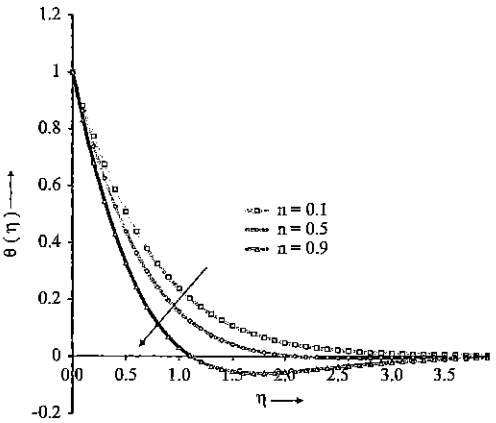

Fig. 12. Thermal stratification effect over the temperature profile when Pr=10.0, *Le*=10.0, *Nb*=0.5, *Nt*=0.5, *S*=2.0, *a*=*ζ*=1.0, *Nr*=0.5, *n*=1.0, *M*=1.0.

seen in the outer boundary region for $n=0.9$ ($Nb=0.5$ and $Nt=0.5$). It is observed that the combined effect of thermophoresis and Brownian motion plays a very dominant role on heat transfer in the presence of thermal stratification.

Fig. 13 illustrates the typical temperature profiles for various values of the radiation parameter N in the presence of nanofluid. At a particular value of N, the temperature decreases with accompanying decreases in the thermal boundary-layer thickness by increasing the values of Pr. Further, it is obvious that for a given Pr, the temperature is decreased with an increase in N. This result can be explained by the fact that a decrease in the values of $(N=4\sigma_1\theta^3/((\rho c_p)_f k^*))$ for given $k*$ and T_∞ means a decrease in the Rosseland radiation absorptive $k*$. According to Eqs. (2) and (3), the divergence of the radiative heat flux $\partial q''_{rad}/\partial y$ increases as $(\rho\ c_p)_f$ decreases which in turn increases the rate of radiative heat transferred to the nanofluid and hence the fluid temperature decreases. In view of this explanation, the effect of radiation becomes more significant as $N\to 0$ ($N\neq 0$) and can be neglected when $N\to\infty$. It is noticed that the temperature decreases with increase of conductive radiation parameter N. The effect of radiation parameter N is to reduce the temperature significantly in the flow region. All these increases in radiation parameter mean the release of heat energy from the flow region and so the fluid temperature decreases as the thermal boundary-layer thickness becomes thicker. All these physical behavior are due to the

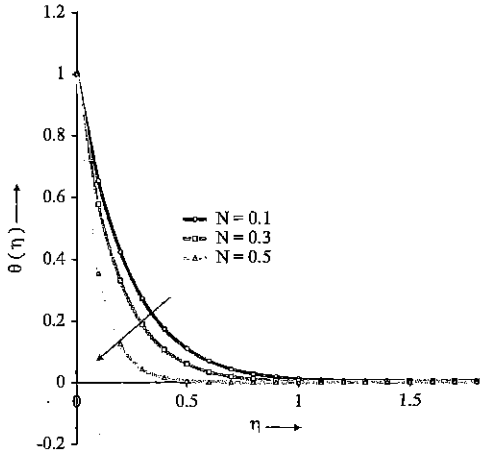

Fig. 13. Effect of conductive radiation over the temperature profile when Pr=10.0, *Le*=10.0, *Nb*=0.5, *Nt*=0.5, *S*=2.0, *a*=1.0, *ζ*=1.0, *Nr*=0.5, *M*=1.0.

combined effects of the strength of thermophoresis particle deposition and the Brownian motion in the nanofluid.

5. Conclusions

Solar radiation caused buoyancy induced flow of an absorbing fluid along an ideally transparent vertical plate embedded in a porosity porous medium was considered. For the nanofluid we employed a model that accounts for the mechanics of the nanoparticle/base-fluid relative velocity by incorporating the effects of Brownian motion and thermophoresis into the governing equations. It is found that the volume fraction of nanoparticles is a key parameter for studying the effect of nanoparticles on flow fields and temperature distributions. It is observed that the numerical solution is possible only when the fluid suction/injection velocity profile varies as $x^{-(1/4)}$. It is interesting to note that the impact of thermophoresis particle deposition with Brownian motion in the presence of thermal stratification have a substantial effect on MHD boundary-layer flow field and, thus, on the heat transfer and nanoparticle volume fraction rate from the sheet to the fluid. Particularly, due to the uniform conduction radiation, the temperature of the fluid increases whereas the nanoparticle volume fraction decreases with increase of Brownian motion. Brownian motion of nanoparticles at the molecular and nanoscale levels is a key nanoscale mechanism governing their thermal behavior. In nanofluid systems, due to the size of the nanoparticles Brownian motion and thermophoresis in the presence of thermal stratification takes place which can affect the heat transfer properties. The increase in radiation parameter means the release of heat energy from the flow region and so the fluid temperature decreases as the thermal boundary-layer thickness becomes thicker. Nanoparticles also offer the potential of improving the radiative properties of the liquids, leading to an increase in the efficiency of direct absorption solar collectors. In the presence of uniform radiation, it is found that with the increase of the magnetic parameter, the momentum boundary-layer thickness decreases, while the thermal boundary-layer thickness increases.

The natural convection of nanofluid, small-particles suspensions has been used in many applications in solar collectors. The present study is of immediate interest in next-generation solar film collectors, heat exchangers technology, materials processing exploiting vertical surfaces, geothermal energy storage and all those processes which are highly affected with heat enhancement concept. The analysis has helped engineers understand the mechanisms that are most important in the deposition process.

One of the technological applications of nanoparticles that hold enormous promise is the use of heat transfer fluids containing suspensions of nanoparticles to confront cooling problems in thermal systems. Hence, the combined effect of thermophoresis particle deposition with Brownian motion on nanofluids due to solar radiation is of great interest worldwide for basic and applied research.

Acknowledgment

The authors wish to express their cordial thanks to our beloved The Vice Chancellor and The Dean, FSSW, UTHM, Malaysia for their encouragements.

References

[1] Nakayama Akira, Koyama Hitoshi. Similarity solutions for buoyancy induced flows over a non-isothermal curved surface in a thermally stratified porous medium. Appl Sci Res 1989;46:309–14.
[2] Batchelor GK. An Introduction to Fluid Dynamics. London: Cambridge University Press; 1987.
[3] Brewster MQ. Thermal radiative transfer properties. John Wiley & Sons; 1972.
[4] Brenner H, Bielenberg JR. A continuum approach to phoretic motions: thermophoresis. Physica A 2005;355:251–73.
[5] Buongiorno J, Hu W. Nanofluid coolants for advanced nuclear power plants. Paper no. 5705. In: Proceedings of ICAPP '05, Seoul; 15–19 May 2005.
[6] Buongiorno J. Convective transport in nanofluids. ASME J Heat Transfer 2006;128:240–50.
[7] Cheng P, Minkowycz WJ. Free convection about a vertical flat plate embedded in a porous medium with application to heat transfer from a dike. J Geophys Res 1977;82:2040–4.
[8] Choi S. Enhancing thermal conductivity of fluids with nanoparticle. In: Siginer DA, Wang HP, editors, Developments and applications of non-Newtonian flows, ASME MD, vol. 231 and FED, vol. 66; 1995. p. 99–105.
[9] Clausing A. Analysis of convective losses from cavity solar central receivers. Solar Energy 1981;27:295–300.
[10] Dehghan AA, Behnia M. Combined natural convection conduction and radiation heat transfer in a discretely heated open cavity. ASME J Heat Transfer 1996;118:54–6.
[12] Gill S. A process for the step-by-step integration of differential equations in an automatic digital computing machine. Proc Cambridge Philos Soc 1951:47 (1);96–108.
[13] Gorla RSR, Sidawi I. Free convection on a vertical stretching surface with suction and blowing. Appl Sci Res 1994;52:247–57.
[14] Kennedy CE. Review of mid- to high-temperature solar selective absorber materials, NREL/TP-520-31267; 2002.
[15] Khan WA, Pop I. Boundary-layer flow of a nanofluid past a stretching sheet. Int J Heat Mass Trans 2010;53:2477–83.
[16] Khlebtsov NG, Trachuk LA, Mel'nikov AG. The effect of the size, shape and structure of metal nanoparticles on the dependence of their optical properties on the refractive index of a disperse medium. Opt Spectrosc 2005;98:77–83.
[17] Kuznetsov AV, Nield DA. Natural convective boundary-layer flow of a nanofluid past a vertical plate. Int J Thermal Sci 2010;49:243–7.
[18] Kuznetsov AV, Nield DA. Natural convective boundary-layer flow of a nanofluid past a vertical plate. Int J Thermal Sci 2009. http://dx.doi.org/10.1016/j.ijthermalsci.2009.07.015.
[19] Kuznetsov AV, Nield DA. Double-diffusive natural convective boundary layer flow of a nanofluid past a vertical plate. Int J Thermal Sci 2011;50:712–7.
[20] Nield DA, Kuznetsov AV. The Cheng-Minkowycz problem for the double-diffusive natural convective boundary layer flow in a porous medium saturated by a nanofluid. Int J Heat Mass Trans 2011;54:374–8.
[21] Ling JX, Dybbs A. Forced convection over a flat plate submersed in a porous medium: variable viscosity case. Paper 87-WA/HT-23. New York: American Society of Mechanical Engineers; 1987.
[22] Masuda H, Ebata A, Teramae K, Hishinuma N. Alteration of thermal conductivity and viscosity of liquid by dispersing ultra-fine particles. Netsu Bussei 1993;7:227–33.
[23] Muftuoglu A, Bilgen E. Heat transfer in inclined rectangular receivers for concentrated solar radiation. Int Commun Heat Mass Trans 2008;35:551–6.
[24] Nield DA, Kuznetsov AV. The Cheng-Minkowycz problem for natural convective boundary layer flow in a porous medium saturated by a nanofluid. Int J Heat Mass Transfer 2009;52:5792–5.
[25] Odeh SD, Behnia M, Morrison GL. Performance evaluation of solar thermal electric generation systems. Energy Convers Manage 2003;44:2425–43.
[26] Richard KS, Lee SM. 800 hours of operational experience from a 2 kW solar dynamic system. In: Space technology and application international forum, Mohamed S El-Genk; 1999. p. 1426–31.
[27] Otanicar Todd P, Phelan Patrick E, Golden Jay S. Optical properties of liquids for direct absorption solar thermal energy systems. Solar Energy 2009;83: 969–977.
[28] Trieb F, Nitsch J. Recommendations for the market introduction of solar thermal power stations. Renew Energy 1998;14:17–22.
[29] Tzou DY. Thermal instability of nanofluids in natural convection. Int J Heat Mass Trans 2008;51:2967–79.
[30] Yurusoy M, Pakdemirli M. Symmetry reductions of unsteady three-dimensional boundary layers of some non-Newtonian Fluids. Int J Eng Sci 1997;35(2):731–40.
[31] Yurusoy M, Pakdemirli M. Exact solutions of boundary layer equations of a special non-Newtonian fluid over a stretching sheet. Mech Res Commun 1999;26(1):171–5.
[32] Yurusoy M, Pakdemirli M, Noyan OF. Lie group analysis of creeping flow of a second grade fluid. Int J Non-linear Mech 2001;36(8):955–60.
[33] Wang CY. Free convection on a vertical stretching surface. ZAMM 1989;69: 418–20.